Wool fibres functionalised with a silane-based coupling agent for reinforced polypropylene composites

Lucia Conzatti [a,*], Francesco Giunco [a], Paola Stagnaro [a], Alessia Patrucco [b], Claudio Tonin [b], Claudia Marano [c], Marta Rink [c], Enrico Marsano [d,*]

[a] *Istituto per lo Studio delle Macromolecole (ISMAC), Consiglio Nazionale delle Ricerche, UOS Genova, Via De Marini 6, 16149 Genova, Italy*
[b] *Istituto per lo Studio delle Macromolecole (ISMAC), Consiglio Nazionale delle Ricerche, UOS Biella, Corso G. Pella 16, 13900 Biella, Italy*
[c] *Dipartimento di Chimica, Materiali ed Ingegneria Chimica, Politecnico di Milano, Piazza L. da Vinci 32, 20133 Milano, Italy*
[d] *Dipartimento di Chimica e Chimica Industriale, Università di Genova, Via Dodecaneso 31, 16146 Genova, Italy*

Received 3 July 2013
Received in revised form 31 January 2014
Accepted 6 February 2014
Available online 14 February 2014

1. Introduction

Protein fibre by-products from the textile industry, waste wool from farms and butchery, and poultry feathers generate a large waste biomass stream that is not subject to adequate forms of valorisation. Nevertheless, using protein fibres to reinforce polymer-based composites for new commodities and/or value-added applications may exploit this untapped resource. Protein fibres are naturally hydrophilic, fire-resistant, biodegradable, biocompat-ible and renewable in addition to exhibiting mechanical or chemical processability [1–9].

In the last decade, the valorisation of short fibres from poultry feathers for reinforcing polyolefin- and polylactide-based composites has been investigated [5,10]. Multi-step pulverisation technologies have been developed to produce ultra-fine ground wool [11,12] as an additive for polypropylene (PP)-based films produced through extrusion and compression moulding. However, the mechanical properties of the obtained materials decline significantly as the wool powder content increases [2]. Another work revealed that wool fibrils can act as a matrix reinforcement increasing the material modulus and yield stress, even though the elongation at break resulted consistently decreased [13]. In a more recent study, silk/wool hybrid fibre PP composites [14] were produced by simple compression moulding and suggested as potential substitutes for the conventional glass/epoxy composites used as electrical insulating materials in printed circuit boards be-cause these composites have characteristically low thermal conductivity.

Isotropic composites based on commercial PP containing up to 60 wt.% highly dispersed wool fibres were prepared using a simple melt blending process and a maleinised PP as a compatibiliser [4]. Although improvements in the thermal stability and elastic modulus were observed, and the presence of the compatibiliser was beneficial, the composites were weaker with respect to the polyolefinic matrix partially because the fibres are shortened dur-ing the melt blending process. Therefore, optimising the process conditions to reduce wool fibre fragmentation and improving the fibre/matrix adhesion are critical for producing materials with a better performance.

The hydrophilicity of the natural fibres adversely affects their adhesion to the hydrophobic PP matrix. For cellulosic fibres, sev-eral chemical methods for modifying their surfaces, such as graft polymerisation using monomers and macromonomers, and the use of suitable coupling agents were proposed in the literature [10,15–19]. Coupling agents, such as maleic anhydride copolymers,

* Corresponding authors. Tel.: +39 0106475866; fax: +39 0106475880 (L. Conzatti). Tel.: +39 0103538727; fax: +39 0103538733 (E. Marsano).
E-mail addresses: conzatti@ge.ismac.cnr.it (L. Conzatti), marsano@chimica.unige.it (E. Marsano).

isocyanates and silanes, can bridge the interface between the fibrous reinforcement and the polymer matrix. Silanes have versatile multifunctional structures and have been successfully applied in polymer composites reinforced with inorganic fillers [20–26] and natural fibres [10,15,17–19,27]. Chemically modifying keratin-based fibres modifies their dye affinity, reduces felting, and improves their wettability in textile wet processing [28–31]. However, to the best of our knowledge, no articles have reported silanising wool fibres and using them to prepare polymer-based composites.

In this work, wool fibres were functionalised with a silane-based coupling agent that might react with both the fibres and the matrix during the mixing process to improve the fibre/matrix adhesion. A silane bearing only one reactive methoxy group was also tested to verify the effectiveness of the silanisation reaction onto the fibres.

PP-based composites containing 20 wt.% of silanised wool fibres were then prepared via melt blending: their morphology was investigated by SEM imaging while their thermal and mechanical behaviour was investigated using thermogravimetric analysis (TGA) and uniaxial tensile tests, respectively. The new materials were compared to composites containing pristine or oxidised wool fibres to evaluate the efficiency of the fibre treatment. The data from mechanical analysis were also compared with theoretical models and the mechanical characteristics of analogous composites containing PP and uncut aligned wool fibres.

2. Experimental

2.1. Materials

Polypropylene *Moplen® HP520H* (PP) with a 0.9 g/cm^3 density and 2 g/10 min melt flow index at 230 °C, 2.16 kg (ISO1133) was supplied in the pellet form by Lyondellbasell Industries S.r.l. (Ferrara, Italy). A polypropylene grafted with maleic anhydride, *Compoline® CO/PP C05* (C05) with 3 g/10 min melt flow index at 230 °C, 2.16 kg (ISO1133), was supplied by Auserpolimeri S.r.l. (Lucca, Italy), and used as a compatibiliser. Wool fibres (WF) in the form of slivers 18 μm in diameter were supplied by The Woolmark Co., Italy. Before mixing, the WF were cut into snippets approxi-mately 2 cm long, washed in a Soxhlet extractor with acetone for 2 h and dried under vacuum at 105 ° C for 4 h. [3-(methacryloyloxy)propyl]trimethoxysilane (MPTS) from Evonik Industries AG (Rheinfelden, Germany) and methoxy(dimethyl)octadecylsilane (MDOS) from Sigma–Aldrich S.r.l. (Milano, Italy) were used as received as coupling agents. Other chemicals were purchased from Sigma–Aldrich.

2.2. Modification of wool fibres

Oxidation. Oxidised wool fibres (WFO) were prepared by using hydrogen peroxide. WF were soaked in a pre-heated (60 °C) aqueous solution containing 0.54 wt.% of hydrogen peroxide, 0.1 g/L of nonylphenol and 2 g/L of sodium pyrophosphate; the mixture was maintained for 2 h at the same temperature. Finally, the fibres were washed with distilled water and dried at 60 °C for 24 h.

Silanisation. Silane-treated wool fibres were prepared from WF or WFO. The silane (typically 10 wt.% relative to the fibres) was dissolved in methanol–water–acetic acid (75/8/17 v/v/v) at 25 °C with continuous stirring for 10 min. The fibres were moistened with the silane-containing mixture and dried at 60 °C for 24 h. The silanisation reaction was completed after raising the temperature to 120 °C for 2 h. Afterward, the wool fibres were treated with ace-tone via Soxhlet and dried to remove unreacted silane.

The effective acetone solubility of the two silanes and the product obtained after self-polymerising the MPTS for 2 h at 120 °C was previously verified.

For the WFO silanised with MPTS, various silane/fibre ratios (3, 6, 10 wt.%) were tested.

2.3. Preparation of the composites

Based on the results obtained by the authors in a previous paper [4], a PP/C05 95/5 wt/wt blend (PPC05) was used as a matrix and a reference. The PPC05 blend was obtained under the same experimental conditions used to prepare the composites. Composites containing 20 wt.% wool fibres (WF, WFO or WFO treated with 10 wt.% MPTS) were prepared via melt blending with a W50 EHT Plasti Corder® (Brabender) internal mixer. PP and C05 pellets (95/5 wt/wt) were introduced in the mixer chamber at 170 °C and mixed (60 rpm rotor speed) for approximately 1 min; the fi-bres were then quickly added and mixing was completed in 10 min (total).

After mixing, all the samples were moulded using a P 200E semi-automatic laboratory press (Collin GmbH) at 180 ° C (5 min at 0.5 MPa and 5 min at 18 MPa) to obtain 0.32 mm thick sheets suitable for characterisation.

Samples with a single fibre were used to measure the critical length (L_c) of the wool fibres into the PPC05 matrix (see below) and were prepared by compression moulding (5 min at 0.5 MPa and 5 min at 18 MPa) a slightly stretched uncut fibre (>8 cm long) between two 0.05 mm thick PPC05 sheets at 180 °C.

Composites containing uncut oriented wool fibres (unidirectional composites) were also prepared by placing combed and slightly stretched WF between two 0.3 mm thick PPC05 sheets and moulding them at 180 °C (5 min at 0.1 MPa and 5 min at 3 MPa). Unidirectional composites with 14.3, 15.7 and 16.6 wt.%wool contents were prepared using WF, WFO and WFO modified with 10 wt.% MPTS (WFO_{10MPTS}), respectively.

2.4. Characterisation

The Fourier transform infrared (FTIR) analyses of MPTS, MDOS and treated wool fibres were performed using a Bruker IFS 28 FTIR spectrophotometer in transmission mode. The liquid silanes were characterised by spreading a drop on a KBr window; for wool fibres, the KBr method was used.

Thermogravimetric analysis (TGA) was carried out with a TGA7 (Perkin Elmer) instrument on samples of approximately 7 mg. The decomposition temperatures at 5 and 50 wt.% mass loss (T_5 and T_{50}, respectively) of the composites were measured while heating at 20 ° C/min under O_2 (35–880 ° C) at 40 mL/min. TGA analyses of the pristine and treated wool fibres were also performed under the same conditions as the composites. The grafted silane content (wt. %) was obtained using the value of the residue at 880 ° C, that corresponds to the amount of SiO_2 formed upon silane combustion:

$$\text{Grafted silane}(\text{wt.}\%) = \frac{SiO_2(\text{wt.}\%)}{FW_{SiO_2}} \cdot FW_{\text{Grafted silane}} \quad (1)$$

where SiO_2 (wt.%) is the residue at 880 °C, FW_{SiO2} and $FW_{\text{Grafted silane}}$ are the formula weights of SiO_2 and the grafted silane moiety, respectively.

For each composite sample, the length and diameter of at least 150 wool fibres were measured using a Polyvar Pol (Reichert) optical microscope equipped with a CCD camera. Because the fibres were tangled, their concentration in the composites was reduced via dilution with neat PP; i.e. each composite sheet was pressed between two PP films to obtain very thin films with few fibre overlaps.

The critical length (L_c) for various matrix/fibre pairs was evaluated according to the "single fibre fragmentation test" (SFFT) [32–36]: a specimen containing a single aligned wool fibre, embedded into the polymer matrix, is stretched along the fibre axis direction until all fragments are shorter than the length needed to transfer sufficient stress from matrix to fibre to break the fibre. The average length of the resulting fibre fragments ($\bar{L}_m$) is correlated to L_c using Eq. (2) [35]:

$$L_c = \frac{4}{3}\bar{L}_m \quad (2)$$

Toward this purpose, 8 cm × 1 cm specimens (0.1 mm thick) with one single wool fibre in a PPC05 matrix were prepared as previously described; uniaxial tensile tests at constant nominal strain rates ($\dot{\varepsilon} = 0.2\ \text{min}^{-1}$) were performed at room temperature with an Instron 5565 dynamometer. After observing the length of wool fibre fragments in specimens loaded until different deformation, the fibre fragmentation tests were finally conducted until ε = 6 to ensure that the shortest length was reached. The length of the obtained wool fibre fragments was then measured using a Polyvar Pol (Reichert) optical microscope.

Scanning electron microscopy (SEM) was performed with a LEO (Leica Electron Optics) 135 VP SEM, at a 15 kV acceleration voltage and a 11 mm working distance. The samples were mounted on aluminium specimen stubs with double-sided adhesive tape and sputter-coated with a 20 nm of gold in rarefied argon using an Emitech K 550 Sputter Coater at 20 mA for 180 s. Cross sections of the films were obtained using fragile fracture in liquid nitrogen.

Energy dispersive X-ray analysis (EDX) of the WFO_{10MPTS} cross sections was carried out with a LEO 1450 VP SEM coupled with an EDX probe operating at 20 kV. Toward this purpose, the fibres were embedded in a PP matrix.

Uniaxial tensile tests at constant nominal strain rate ($\dot{\varepsilon} = 0.29\ \text{min}^{-1}$) were performed at room temperature and 50%relative humidity with a displacement-controlled dynamometer (Instron 1121 or S Series Housenfield). A video-extensometer was used for the strain measurements. For the wool fibres, the nominal strain was $\varepsilon_{nom} = \Delta L/L_0$, where ΔL is the overall displacement and L_0 is the initial fibre length (20 mm).

3. Results and discussion

3.1. Treatment of wool fibres

Previous results regarding PP- and PPC05-based composites containing different WF contents [4] indicated that using maleinised polypropylene (C05) as a compatibiliser improves the fibre–matrix interactions. In this work, to enhance the adhesion between the wool fibres and the polyolefinic matrix, WF were modified with a silane coupling agent using a slightly modified literature procedure [27].

[3-(Methacryloyloxy)propyl]trimethoxysilane (MPTS) is a cost effective silane able to react with PP during mixing; it was chosen as a coupling agent. To favour the reaction with MPTS, WF were oxidised (WFO) to generate new chemical functionalities, such as —SO_3H and —COOH, on the WF surface [37]. The initial MPTS concentration was varied (3, 6 and 10 wt.%) to evaluate the effect on the amount of silane grafted onto the fibres.

As known [17,38], the interaction between a silane coupling agent and natural fibres proceeds through several steps: (i) hydrolysis of the silane, yielding the reactive silanol groups; (ii) physical adsorption of the reactive silane onto the natural fibres; and (iii) conversion, upon heating, of the hydrogen bonds formed between the silanols and the hydroxyl groups borne by fibres into covalent —Si—O—C— bonds via water condensation.

However, due to steric reasons, it is impossible for all the three silanol groups on the MPTS molecule to react with the natural fibres. Consequently, the residual silanol groups can self-condense, forming polysiloxanic structures with stable —Si—O—Si— bonds that may wrap the fibres.

To verify the reaction between the silane and the fibres, WF and WFO were treated with methoxy(dimethyl)octadecylsilane (MDOS) bearing only one reactive methoxy group.

The wool fibres obtained after treatment with MPTS and MDOS (Scheme 1) were extracted with acetone via Soxhlet to remove any unreacted silane and/or polysiloxane formed from MPTS self-condensation that were not chemically linked or physically entangled to the fibres. The FTIR spectra (not shown) exhibit a series of peaks indicating the presence of silane and/or polysiloxane in the extracts.

The presence of the silane on the fibres and the modifications to the fibre surface morphology were assessed using SEM.

The cell structure of wool fibres is characterised by the presence of three main morphological components: the cuticle, the cell membrane complex and the cortex. The cuticle consists of a thin layer of flat overlapping "cuticle cells" surrounding the fibre; cuticle cells are cemented to the fibre bulk (cortex) via the cell membrane complex sometimes referred to as intercellular cement. Fig. 1a displays the cuticle morphology of an untreated wool fibre: the cuticle cells are flat, thin, and adhered to the fibre bulk.

Relative to pristine WF, the fibres treated with both MPTS (Fig. 1b) and MDOS (Fig. 1c) display the thickening and increased detachment of cuticle cells from the fibre bulk, suggesting that the silane treatment primarily affects the cell membrane complex; this selectivity might occur because in wool, the hydrophobic external layer (the epi-cuticle) surrounding each cuticle cell re-mains intact and the reaction is selective for the cell membrane complex zone that extends across the fibre surface. The cell mem-brane complex is less cross-linked (1% half cystine) and more reac-tive relative to the epi-cuticle (12% half cystine) [39] and therefore swells after reacting with the silane thus raising the cuticle cells.

Obvious degradation on the cuticle surface occurs after oxidising the wool, while the corresponding chemical functionalities (—SO_3H, —COOH) are activated toward the silane methoxy groups [37]. The surface morphologies of WFO, WFO treated with 10 wt.% MDOS and increasing amounts (3, 6 and 10 wt.%) of MPTS were compared in Fig. 2. The SEM image in Fig. 2a confirmed that the cuticle cells were dramatically modified after the wool oxidation (compare Fig. 1a with Fig. 2a). The oxidised fibres treated with MPTS, aside from the morphological features already observed in the analogously treated WF, also display a wrinkled cuticle surface due to the activation of the protein substrate during the oxidative treatment (Fig. 2b–d). The thin silane coating formed on the surface progressively increases the thickness and detachment of the cuticle cells, as well as the polymer aggregation on the fibre surface, when increasing the MPTS concentration. Therefore, MPTS reacts with the cell membrane complex and the epi-cuticle of WFO. The Si atoms were present along the wool fibre radius, as con-

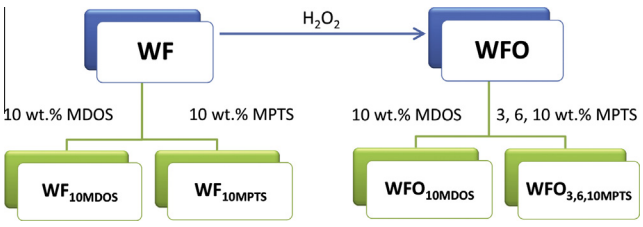

Scheme 1. Wool fibres obtained after treatment with MPTS and MDOS silanes.

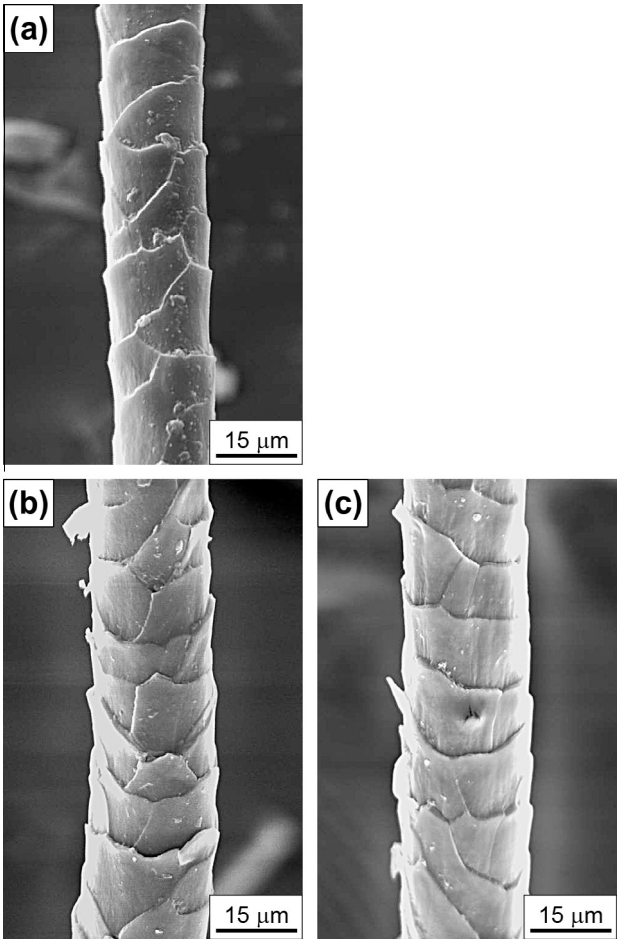

Fig. 1. SEM (1000×) images of WF (a) and WF treated with 10 wt.% MPTS (b) and 10 wt.% MDOS.

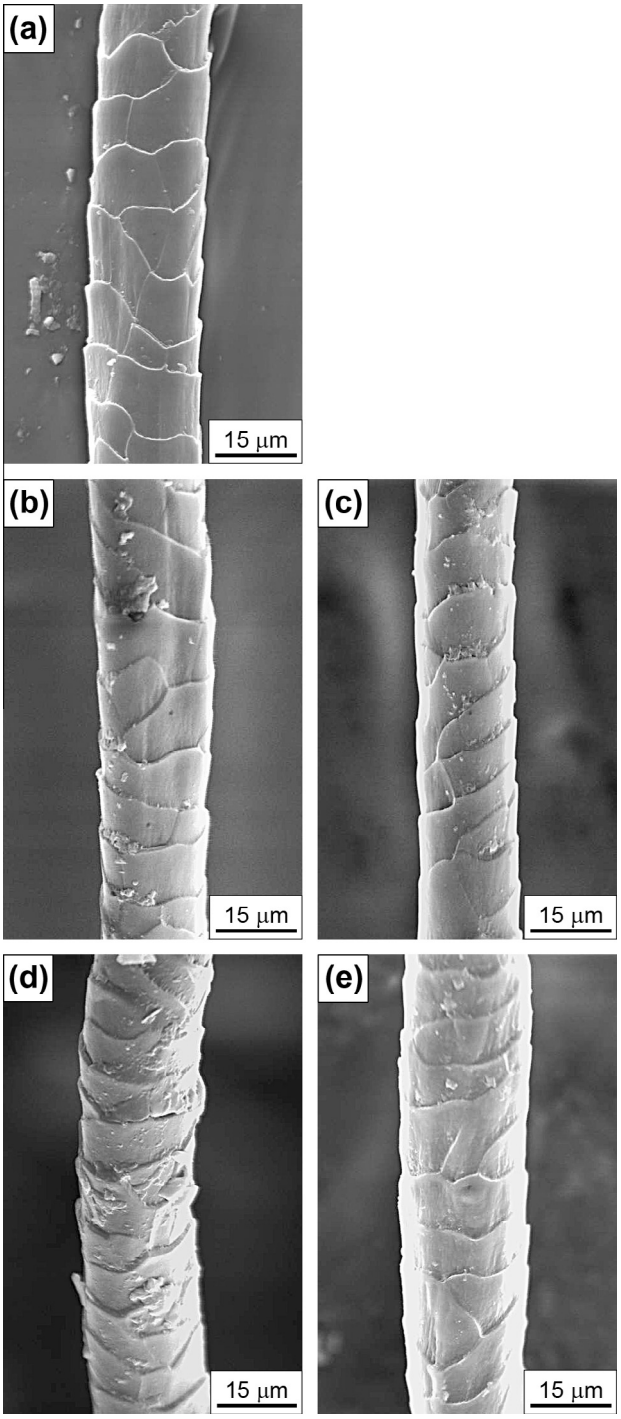

Fig. 2. SEM (1000×) images of WFO (a) and WFO treated with 3 wt.% MPTS (b), 6 wt.% MPTS (c), 10 wt.% MPTS (d), and 10 wt.% MDOS (e).

firmed by SEM–EDX analysis of the WFO_{10MPTS} cross sections displayed in Fig. 3.

The reaction occurred across the entire fibre surface when the WFO were treated with MDOS (Fig. 2e); MDOS has one methoxy group, precluding self-polymerisation and ensuring reaction with the wool.

The presence of the silane onto fibre surface after solvent extraction was also assessed using FTIR spectroscopy. The resultant spectra for the MPTS, WFO and WFO_{10MPTS} are compared in Fig. 4. The spectrum of neat MPTS (trace a of Fig. 4) exhibits the sharp peak at 1714 cm^{-1} due to the stretching mode of the C═O from the methacrylate group and two peaks at approximately 1635 and 1450 cm^{-1} ascribed to the stretching mode of the C═C bond and the deformation mode of the —CH_2— groups of the silane, respectively. By comparing the FTIR spectra of WFO_{10MPTS} (trace c in Fig. 4) to that of WFO (trace b in Fig. 4) some differences are evi-dent: the intensity of the bands related to the —CH_3 and —CH_2— groups (2952 and 2890 cm^{-1}, respectively) slightly increases, a sharp peak appears at 1714 cm^{-1} and the region between 900 and 1400 cm^{-1}, where the stretching bands of —Si—O—R— and —Si—O—Si— groups are commonly observed, is slightly modified. The FTIR findings confirm the presence of silane on the MPTS-trea-ted fibres after extraction, validating the SEM analysis.

A similar indication was found from the FTIR analysis of extracted WFO_{10MDOS}, even though the spectrum of MDOS (trace a of Fig. 5) does not present obvious bands in the clear regions of the WFO spectrum. The close comparison between the WFO and WFO_{10MDOS} spectra (respectively traces b and c of Fig. 5) reveals a difference in the relative intensity of the bands in the 2850–2950 cm^{-1} region that correspond to the stretching modes of the —CH_2— and —CH_3 groups. In particular, after the reaction with the wool fibres, the band at approximately 2920 cm^{-1} appears more intense than that at approximately 2950 cm^{-1}.

To determine the amount of silane present on the treated fibres, TGA analyses under O_2 were performed (Table 1). The amount of grafted silane was evaluated by using Eq. (1); this equation accounts for the residue at 880 °C obtained from treated fibres. This residue is SiO_2 generated from silane combustion [40], because neither WF nor WFO exhibit any residue under these conditions.

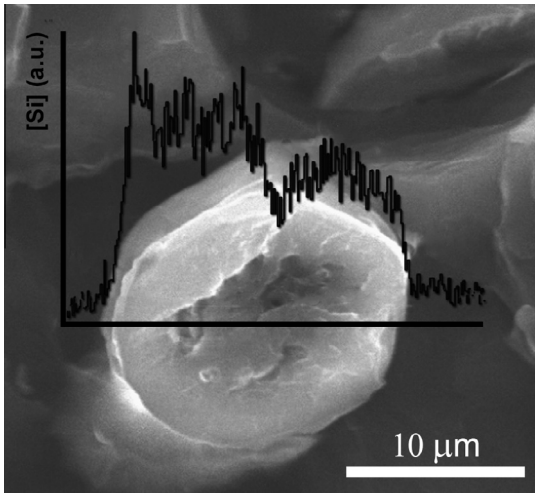

Fig. 3. EDX analysis of Si carried out by SEM imaging of the WFO_{10MPTS} cross sections.

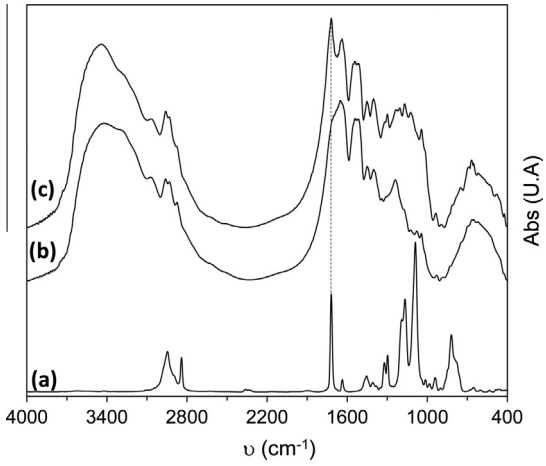

Fig. 4. Comparison of the FTIR spectra obtained for MPTS (a), WFO (b) and WFO_{10MPTS} (c).

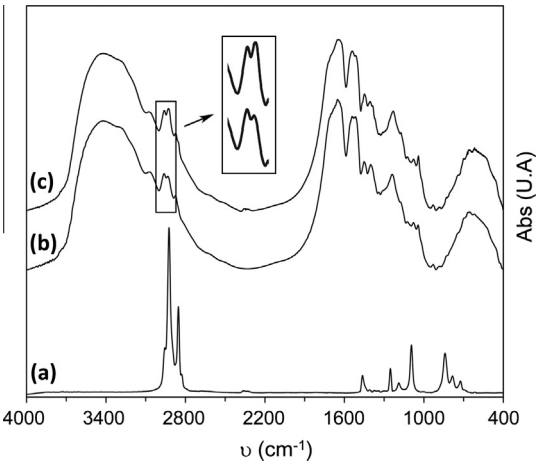

Fig. 5. Comparison of the FTIR spectra obtained for MDOS (a), WFO (b) and WFO_{10MDOS} (c).

The experimental results obtained for samples 1 and 2 indicate that the MDOS molecules preferentially react with the oxidised wool fibres. When using the same initial concentration of silane (10 wt.%), less grafted MDOS is present on the WF (sample 1, 0.4 wt.%) than on WFO (sample 2, 4.6 wt.%).

Table 1
Amounts of grafted silane obtained during TGA analysis under O_2 for untreated and treated wool fibres.

Sample	Fibre	Silane	C_o[a]	SiO_2 at 880 °C[b]	Grafted silane[c]	
			(wt.%)	(wt.%)	(wt.%)	(mmol/100 g)
1	WF	MDOS	10	0.1	0.4	1.2
2	WFO	MDOS	10	0.9	4.6	14.7
3	WFO	MPTS	10	1.7	5.7	29.5
4	WFO	MPTS	6	1.0	3.4	17.2
5	WFO	MPTS	3	0.6	1.9	9.4

[a] Concentration of silane with respect to the fibre used for wool treatment.
[b] SiO_2 residue obtained at 880 °C.
[c] Amount of grafted silane evaluated by using Eq. (1).

The amount of MPTS silane grafted onto WFO is higher than that observed for MDOS due to self-condensation of the unreacted silanols on the grafted MPTS molecules to form polysiloxane chains. Although most of the polysiloxane chains were extracted with acetone, some of them, even without a chemical bond to the fibres, might not be easily extractable due their physical entanglement.

The amount of silane grafted onto the fibres decreases with the initial MPTS concentration. Sample 3 contains WFO modified with the maximum amount of MPTS and was chosen as the treated wool fibre (WFO_{10MPTS}) used to prepare the PPC05-based composites.

3.2. PPC05-based composites containing wool fibres

Homogeneous PPC05-based composites containing 20 wt.% WF, WFO, or WFO_{10MPTS} were successfully prepared by melt compounding in an internal mixer, as described in the Experimental section.

The thermo-oxidative stability of the fibres, the PPC05 matrix and their composites was studied by TGA analysis carried out in dynamic mode under an oxygen atmosphere. The TG curves for both the wool fibres and the composites exhibit a variable weight loss step (up to 10 wt.%) from 35–150 °C that corresponds to the release of the absorbed water and depends on the relative humidity. For comparison, the TG curves were thus rescaled at 100 wt.% starting from 150 °C to eliminate the initial weight variations. From these curves, the decomposition temperatures at 5 and 50 wt.% mass loss (T_5 and T_{50}, respectively) were determined (Table 2).

The fibre treatments slightly affect thermo-oxidative resistance of wool. WFO_{10MPTS} displays a lower T_5 value than both WF and WFO most likely due to the organic moiety on the silane molecule. However, the T_{50} values for both WFO and WFO_{10MPTS} are approximately 20 °C higher than that of WF.

The T_5 values for the PPC05, PPC05/WF and PPC05/WFO composites are similar, while the degradation of the sample containing

Table 2
Thermal parameters obtained during TGA analysis under O_2.[a]

Sample	T_5 (°C)	ΔT_5 [b] (°C)	T_{50} (°C)	ΔT_{50} [b](°C)
WF	267 ± 3		436 ± 3	
WFO	267 ± 3		456 ± 3	
WFO_{10MPTS}	256 ± 3		450 ± 8	
PPC05	271 ± 3	–	322 ± 3	–
PPC05/WF	272 ± 3	0	358 ± 3	36
PPC05/WFO	276 ± 3	5	358 ± 4	36
PPC05/WFO_{10MPTS}	282 ± 3	11	380 ± 6	58

[a] Values obtained from TG curves rescaled at 100 wt.% starting from 150 °C.
[b] Increase of T_5 or T_{50} of the composites with respect to the PPC05 matrix.

WFO_{10MPTS} initiates at higher temperatures. In addition, the T_{50} values of the composites are higher than the values of the neat matrix, particularly when WFO_{10MPTS} is included. The increased thermo-oxidative stability of the composites relative to the polyolefinic matrix might occur not only due to the difference between the degradation temperatures of the fibres and the matrix, but also due to the synergistic effect of the two components. To understand this aspect, theoretical TG curves for composites containing 20 wt.% fibres were obtained by calculating the residual weight percentage of the composite $(W_c)_T$ as a function of the temperature:

$$(W_c)_T = 0.8(W_m)_T + 0.2(W_f)_T \quad (3)$$

where, $(W_m)_T$ and $(W_f)_T$ are the residual weight percentages at a given temperature (T) of the PPC05 matrix and of the different fibres (WF, WFO and WFO_{10MPTS}), respectively, obtained from the individual experimental TG traces of the two components.

From these curves, the theoretical T_5 and T_{50} values (T_{5TH} and T_{50TH}, respectively) were obtained and compared in Fig. 6 with the corresponding experimental values reported in Table 2. For every composite, the experimental values are higher than those predicted using only the addition rules. This effect is more evident in the samples containing the fibres modified with MPTS, suggest-ing a synergistic effect between the two components that could be caused by positive interactions between the fibres and the matrix.

The fibre/matrix adhesion in the prepared composites was evaluated by a SEM investigation of the fragile fractures produced in liquid nitrogen. Fig. 7 displays representative micrographs of the composites. The WF appear separated from one another and homogeneously distributed within the PPC05, but their adhesion to the matrix remains unsatisfactory (Fig. 7a): pulled-out fibres left large voids, cavities and imprints on the polymer fracture surface. The oxidation process does not significantly improve adhesion, as illustrated in Fig. 7b; the cavities and imprints are still evident. In the PPC05/WFO_{10MPTS} sample, fewer voids and cavities around the fibres were observed (Fig. 7c), indicating enhanced fibre/matrix adhesion.

3.3. Reinforcing effect of fibres

The mechanical behaviour of the fibres was studied. Fig. 8a presents the stress–strain curves for WFO and WFO_{10MPTS} reported for comparison with that of the untreated WF. As reported in the Experimental section, the strain was measured as $\Delta L/L_0$, where ΔL is the overall displacement, and L_0 is the initial gauge length. The nominal stress was determined as $\sigma_{nom} = F/A_0$, where F is the

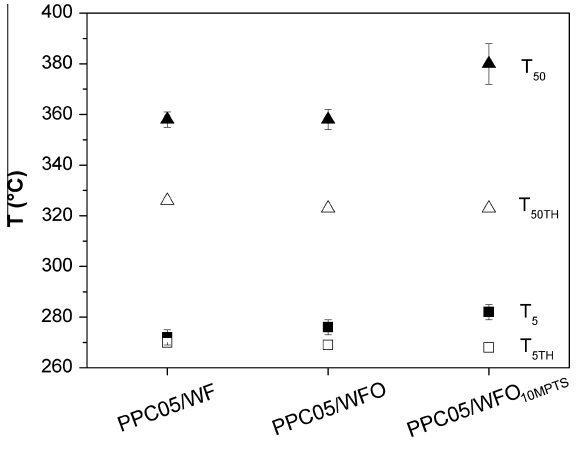

Fig. 6. Theoretical values for T_{5TH} (□) and T_{50TH} (△) compared to the experimental T_5 (■) and T_{50} (▲) values in Table 2.

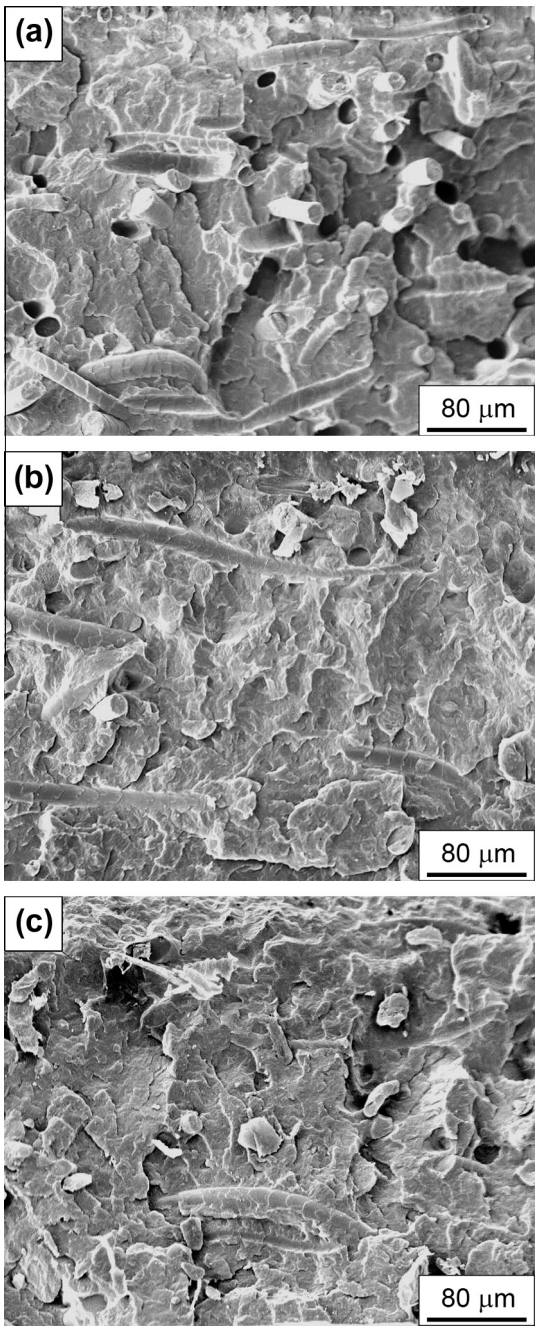

Fig. 7. SEM (200×) cross-sectional images of the PPC05/WF (a), PPC05/WFO (b) and PPC05/WFO_{10MPTS} (c) composites.

applied force and $A_0 = \pi D^2/4$ is the cross-sectional area of the fibre (D is the mean value of the fibre diameter, as measured in the images captured by optical microscopy).

The observed changes in the fibre compliance are usually referred to as wool fibre yielding and have been interpreted in terms of different deformation processes in the complex wool structure [41,42]. The obtained results reveal that treating the fibres does not significantly affect their overall mechanical behaviour; their elastic modulus and strength are almost unchanged, even though the treatment modified the fibres, as observed via SEM. Therefore, the means of the modulus and yield strength were assessed for wool fibres and PPC05 matrix. The PPC05 stress–strain curve is presented in Fig. 8b.

In addition to the adhesion between the fibres and the matrix, the mechanical properties of a composite generally depend also

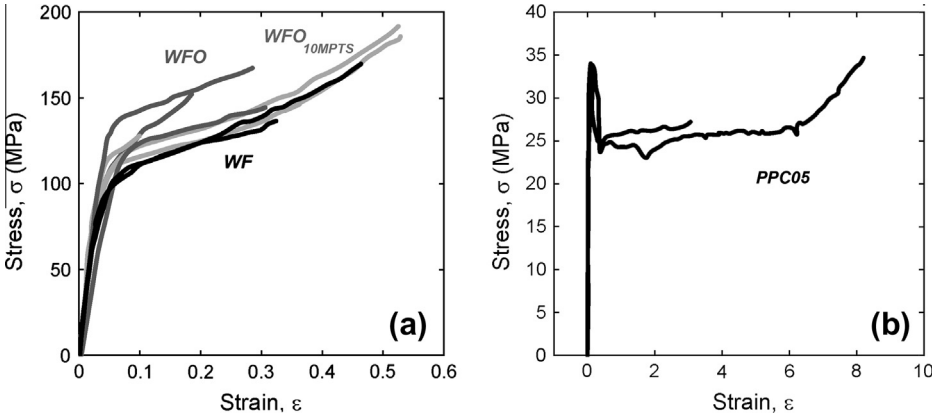

Fig. 8. Stress–strain curves for the WF, WFO and WFO_{10MPTS} (a), as well as the PPC05 matrix (b).

on the orientation and dimensions of the fibres. To obtain the average stress of the fibres in a composite that is as close as possible to the maximum, the fibres should exceed the critical length (L_c). When considering fibres with similar mechanical characteristics, lower L_c values indicate better fibre–matrix interactions [43,44].

L_c was evaluated for the different matrix/fibre pairs as described in the Experimental section; the obtained values are reported in Table 3. The L_c value obtained for WFO_{10MPTS} is the lowest, while that of WF is the highest. This finding further confirms the coupling abilities of the grafted silane molecule in the PPC05 matrix.

Another important parameter affecting the reinforcement of polymer matrices is the fibre length in the final composites. To verify that the wool fibres strengthened the composites, the fibre breakage caused by mixing was studied and the fibre length was measured in every prepared composites. In Table 4, the number ($\bar{L}_n$) and the weight ($\bar{L}_w$) average lengths and the relative polydis-persity index ($\bar{L}_w/\bar{L}_n$) for the fibres was obtained by measuring at least 150 fibres for each sample.

Both oxidation and MPTS treatments improved the breakage resistance of the wool fibres during mixing. In particular, the PPC05/WFO_{10MPTS} composite exhibited the best breakage resis-tance with the highest $\bar{L}_n$ and the most fibres longer than L_c.

Fig. 9 reports the nominal stress–strain curves of the compos-ites containing treated wool fibres in comparison with those using untreated WF. The modulus (E) and strength (yield stress, σ_y) of the materials are also reported in the figure inset. The PPC05/WFO and $PPC05/WFO_{MTPS}$ composites have similar mechanical behaviours regardless of the wool fibre surface treatment. With respect to PPC05/WF, they have higher moduli and strengths, but they break at a lower strain. The increased yield stress observed

Table 3
L_c values obtained for the different matrix/fibre pairs.

Matrix	Fibre	L_c (mm)
PPC05	WF	0.72
PPC05	WFO	0.57
PPC05	WFO_{10MPTS}	0.43

Table 4
Number ($\bar{L}_n$) and weight average ($\bar{L}_w$) fibre length and polydispersity index ($\bar{L}_w/\bar{L}_n$) of the fibres in composites containing untreated and treated wool fibres.

Samples	$\bar{L}_n$ (mm)	$\bar{L}_w$ (mm)	$\bar{L}_w/\bar{L}_n$	WF with $L > L_c$ (%)
PPC05/WF	0.16	0.31	2.00	0.9
PPC05/WFO	0.28	0.46	1.63	15.6
$PPC05/WFO_{10MPTS}$	0.36	0.50	1.39	30.0

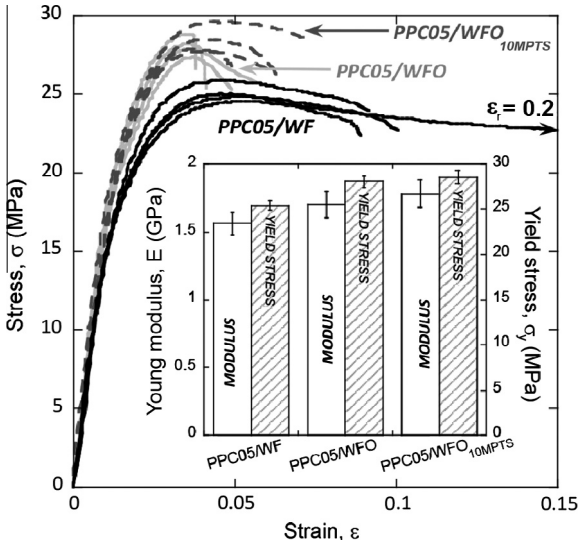

Fig. 9. Stress–strain curves for the PPC05-wool fibre composites.

when the treated wool fibres are used can be related to the increased polymer-fibre adhesion and/or to the increased percentage of fibres with lengths exceeding L_c.

To understand which of these two mechanisms is responsible for the observed increase in the composite strength, samples con-taining uncut aligned fibres (unidirectional composites) were also prepared (see the Experimental section) and characterised. Fig. 10a displays the nominal stress–strain curves of these sam-ples; the actual wool fibres content (wt.%) is also reported. The modulus and yield strength of the same composites are reported in Fig. 10b with those of the PPC05 matrix. The data obtained in a previous paper [4] describing a unidirectional composite based on uncompatibilised PP with 16.6 wt. % of WF are also reported for comparison.

The differences in the E of the PPC05-based composites cannot be ascribed to their different composition because in that case, E should monotonically increase with the wool fibre content. For PPC05/WF, an E value close to that of the matrix was unexpectedly obtained: fibre misalignment might have occurred during composite preparation.

The predicted composite modulus (E_c) and yield stress (σ_c) values were determined according to Eqs. (4) and (5) [45] and are also reported in Fig. 10b.

$$E_c = V_f \cdot E_f + (1 - V_f) \cdot E_m \quad (4)$$

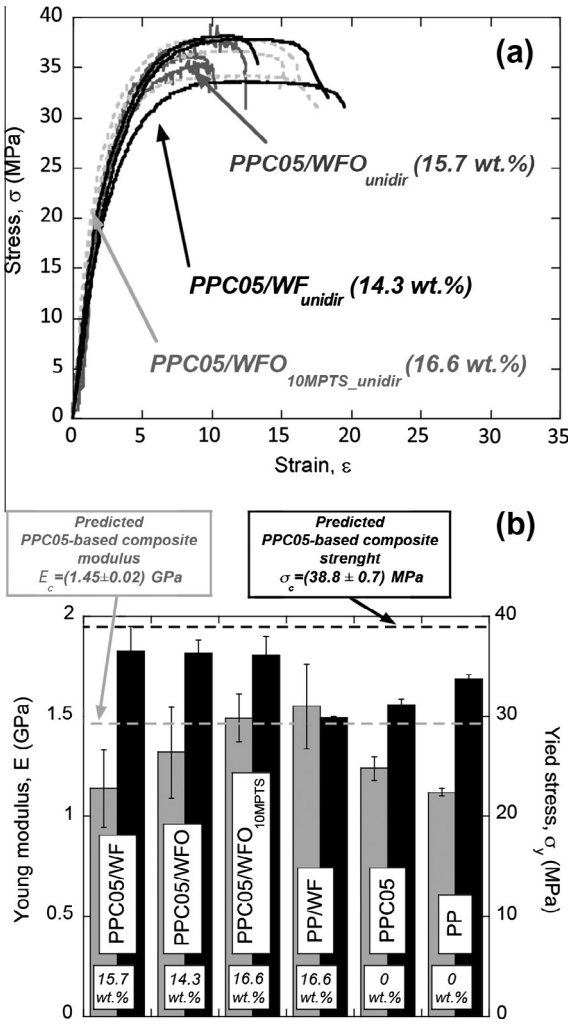

Fig. 10. Composites containing un-cut aligned wool fibres (unidirectional composites): nominal stress–strain curves (a) and material modulus and yield strength (b).

$$\sigma_c = \sigma_{fu} V_f + \sigma'_m (1 - V_f) \quad (5)$$

E_m is the PPC05 modulus (1.24 ± 0.06 GPa); E_f is the wool fibre modulus (3.2 ± 0.4 GPa); V_f is the wool fibres volume fraction (a mean value of 0.11, determined using a density value of 0.9 and 1.33 g/cm^3 for PPC05 and WF, respectively, was used); σ_{fu} is the fibre tensile strength (115 ± 12 MPa); σ'_m is the stress in the matrix at the fibre strain at failure (σ'_m = 29.4 MPa).

The uncertainty reported in the predicted E_c and σ_c values refers to their variations when the highest or the lowest wool content is considered. Except for PPC05/WF, the modulus values for the different PPC05 composites are consistent with those predicted by Eq. (4).

For the composite strength, PPC05-based composites exhibit a higher yield stress than the PPC05 matrix, suggesting there is a good adhesion between polymer and wool. Nevertheless, treating the fibres does not seem to affect the composite strength: similar yield stress values are obtained for both treated and untreated wool fibres. Therefore, the increase in the material resistance observed in the short, treated fibre composites is not to be related to the wool fibre treatment; instead, the effect should be ascribed to the higher percentage of long fibres ($L > L_c$) in the PPC05/WFO and PPC05/WFO$_{10MPTS}$ composites relative to PPC05/WF.

Moreover, because the PPC05/WF composite is more resistant than the corresponding PP-based composite (PP/WF), the increase in the material strength observed when PPC05-based composites are considered must be ascribed to the presence of C05.

4. Conclusions

Silanising pre-oxidised wool fibres with [3-(methacryloyloxy)propyl]trimethoxy silane for polypropylene-based composites was achieved, as confirmed by FTIR and SEM analyses.

Polypropylene-based composites containing 20 wt.% unmodified, oxidised or silanised wool fibres were prepared using a simple melt blending procedure. The morphological investigations performed on fragile fractures revealed that in the composites containing the silanised fibres, the adhesion between the fibres and the polymer matrix was enhanced.

All of the composite materials displayed improved thermo-oxidative stability with respect to the neat polyolefinic matrix and the values predicted by adding the contributions of the single components. This effect is more evident with the silanised fibres.

Analysis of the mechanical behaviour of the composites revealed that the wool fibres exerted a lower than expected reinforcing effect on the polypropylene matrix due to the wool fibre fragmentation during mixing. This fragmentation was alleviated by the silane modification but still generated fibres with lengths that are insufficient for overcoming the critical value of the fibre/matrix pair.

Acknowledgments

The authors gratefully acknowledge the CARIPLO Bank Foundation Project KEBAB 2009–2011 for the financial support and Dr. G. Battilana (CNR-IENI Genova, Italy) for the SEM–EDX analysis of the modified wool fibres.

References

[1] Barone JR, Gregoire NT. Characterisation of fibre–polymer interactions and transcrystallinity in short keratin fibre–polypropylene composites. Plast, Rubber Compos 2006;35(6–7):287–93.
[2] Xu W, Wang X, Li W, Peng X, Liu X, Wang XG. Characterization of superfine wool powder/poly(propylene) blend film. Macromol Mater Eng 2007;292(5):674–80.
[3] Aluigi A, Vineis C, Ceria A, Tonin C. Composite biomaterials from fibre wastes: characterization of wool–cellulose acetate blends. Compos Part A-Appl S 2008;39(1):126–32.
[4] Conzatti L, Giunco F, Stagnaro P, Patrucco A, Marano C, Rink M, et al. Composites based on polypropylene and short wool fibres. Compos Part A-Appl S 2013;47:165–71.
[5] Barone JR, Schmidt WF, Liebner CFE. Compounding and molding of polyethylene composites reinforced with keratin feather fiber. Compos Sci Technol 2005;65(3–4):683–92.
[6] Salhi A, Kaci S, Boudenne A. Development of bio-composites based of polymer matrix and keratin fibers: contribution to poultry biomass recycling. In: Boudenne A, editor. Polymer Composite Materials: From Macro, Micro to Nanoscale. Paris: 2011. p. 237–43.
[7] Barone JR. Lignocellulosic fiber-reinforced keratin polymer composites. J Polym Environ 2009;17(2):143–51.
[8] Barone JR, Schmidt WF. Polyethylene reinforced with keratin fibers obtained from chicken feathers. Compos Sci Technol 2005;65(2):173–81.
[9] Conzatti L, Giunco F, Stagnaro P, Capobianco M, Castellano M, Marsano E. Polyester-based biocomposites containing wool fibres. Compos Part A-Appl S 2012;43(7):1113–9.
[10] Huda MS, Schmidt WF, Misra M, Drzal LT. Effect of fiber surface treatment of poultry feather fibers on the properties of their polymer matrix composites. J Appl Polym Sci 2013;128(2):1117–24.
[11] Xu W, Cui W, Li W, Guo W. Development and characterizations of super-fine wool powder. Powder Technol 2004;140(1):136–40.
[12] Xu W, Guo W, Li W. Thermal analysis of ultrafine wool powder. J Appl Polym Sci 2003;87(14):2372–6.
[13] Liu Y, Yin R, Yu W-D. The bio-inspired study of homogeneous composite materials. J Compos Mater 2011;45(1):113–25.
[14] Rajkumar G, Srinivasan J, Suvitha L. Development of novel silk/wool hybrid fibre polypropylene composites. Iran Polym J 2013;22(4):277–84.
[15] Belgacem MN, Gandini A. The surface modification of cellulose fibres for use as reinforcing elements in composite materials. Compos Interface 2005;12(1–2):41–75.

[16] Shubhra QTH, Alam A, Quaiyyum MA. Mechanical properties of polypropylene composites a review. J Thermoplast Compos 2013;26(3):362–91.
[17] Xie Y, Hill CAS, Xiao Z, Militz H, Mai C. Silane coupling agents used for natural fiber/polymer composites: a review. Compos Part A-Appl S 2010;41(7):806–19.
[18] Huda MS, Drzal LT, Mohanty AK, Misra M. Effect of fiber surface-treatments on the properties of laminated biocomposites from poly(lactic acid) (PLA) and kenaf fibers. Compos Sci Technol 2008;68(2):424–32.
[19] Huda MS, Drzal LT, Mohanty AK, Misra M. Effect of chemical modifications of the pineapple leaf fiber surfaces on the interfacial and mechanical properties of laminated biocomposites. Compos Interface 2008;15(2–3):169–91.
[20] Li Y, Yu J, Guo Z-X. The influence of silane treatment on nylon 6/nano-SiO_2 in situ polymerization. J Appl Polym Sci 2002;84(4):827–34.
[21] Clark HA, Plueddemann EP. Bonding of silane coupling agents in glass-reinforced plastics. Mod Plast 1963;40(10):133–96.
[22] Favis BD, Blanchard LP, Leonard J, Prud'Homme RE. The interaction of a cationic silane coupling agent with mica. J Appl Polym Sci 1983;28(3):1235–44.
[23] Park JM, Subramanian RV, Bayoumi AE. Interfacial shear strength and durability improvement by silanes in single-filament composite specimens of basalt fiber in brittle phenolic and isocyanate resins. J Adhes Sci Technol 1994;8(2):133–50.
[24] Park S-J, Jin J-S. Effect of silane coupling agent on interphase and performance of glass fibers/unsaturated polyester composites. J Colloid Interface Sci 2001;242(1):174–9.
[25] Wu HF, Dwight DW, Huff NT. Effects of silane coupling agents on the interphase and performance of glass-fiber-reinforced polymer composites. Compos Sci Technol 1997;57(8):975–83.
[26] Metın D, Tihminlioğlu F, Balköse D, Ülkü S. The effect of interfacial interactions on the mechanical properties of polypropylene/natural zeolite composites. Compos Part A-Appl S 2004;35(1):23–32.
[27] Herrera-Franco P, Valadez-Gonzalez A. A study of the mechanical properties of short natural-fiber reinforced composites. Compos Part B-Eng 2005;36(8):597–608.
[28] Freddi G, Tsukada M, Shiozaki H. Chemical modification of wool fibers with acid anhydrides. J Appl Polym Sci 1999;71(10):1573–9.
[29] Hess JF, FitzGerald PG. Treatment of keratin intermediate filaments with sulfur mustard analogs. Biochem Biophys Res Commun 2007;359(3):616–21.
[30] Kuzuhara A. Chemical modification of keratin fibers using 2-iminothiorane hydrochloride. J Appl Polym Sci 2003;90(13):3646–51.
[31] Kan CW, Yuen CWM. A comparative study of wool fibre surface modified by physical and chemical methods. Fiber Polym 2009;10(5):681–6.
[32] Bascom WD, Jensen RM. Stress transfer in single fiber/resin tensile tests. J Adhesion 1986;19(3–4):219–39.
[33] Baxevanakis C, Jeulin D, Valentin D. Fracture statistics of single-fibre composite specimens. Compos Sci Technol 1993;48(1):47–56.
[34] Curtin WA. Exact theory of fibre fragmentation in a single-filament composite. J Mater Sci 1991;26(19):5239–53.
[35] Tripathi D, Lopattananon N, Jones FR. A technological solution to the testing and data reduction of single fibre fragmentation tests. Compos Part A-Appl S 1998;29(9–10):1099–109.
[36] Waterbury MC, Drzal LT. On the determination of fiber strengths by in situ fiber strength testing. J Compos Tech Res 1991;13(1):22–8.
[37] Maclaren JA, Milligan B. Wool science. The chemical reactivity of the wool fibre. Marrickville, Australia: Science Press; 1981.
[38] Abdelmouleh M, Boufi S, ben Salah A, Belgacem MN, Gandini A. Interaction of silane coupling agents with cellulose. Langmuir 2002;18(8):3203–8.
[39] Rippon JA. The structure of wool. In: Lewis DM, editor. Wool dyeing. Leeds: Society of Dyers and Colourists; 1992. p. 22.
[40] Larena A, Matias MC, Urreaga JM. Thermal degradation of polysiloxane coatings on E-glass fiber. A FTIR study. Spectrosc Lett 1992;25(7):1121–9.
[41] Blackburn S, Lindley H, Burte H, Harris M, Mizel L, Fourt L, et al. Physical properties of wool fibres. In: Secretariat TIW, editor. Wool Science Review; 1955. p. 27–38.
[42] Tsobkallo K, Aksakal B, Darvish D. Analysis of the contribution of the microfibrils and matrix to the deformation processes in wool fibers. J Appl Polym Sci 2012;125(S2). E168–E79.
[43] Kelly A, Tyson WR. Tensile properties of fibre-reinforced metals: copper/tungsten and copper/molybdenum. J Mech Phys Solids 1965;13(6):329–50.
[44] Van den Oever MJA, Bos HL, Van Kemenade M. Influence of the physical structure of flax fibres on the mechanical properties of flax fibre reinforced polypropylene composites. Appl Compos Mater 2000;7(5–6):387–402.
[45] Harris B. Engineering composite materials. London: IOM; 1999.